



UNIVERSITÀ POLITECNICA DELLE MARCHE  
Repository ISTITUZIONALE

Development of a measurement setup to detect the level of physical activity and social distancing of ageing people in a social garden during COVID-19 pandemic

This is the peer reviewed version of the following article:

*Original*

Development of a measurement setup to detect the level of physical activity and social distancing of ageing people in a social garden during COVID-19 pandemic / Casaccia, S.; Naccarelli, R.; Moccia, S.; Migliorelli, L.; Frontoni, E.; Revel, G. M.. - In: MEASUREMENT. - ISSN 0263-2241. - 184:(2021).  
[10.1016/j.measurement.2021.109946]

*Availability:*

This version is available at: 11566/291648 since: 2024-11-18T11:15:24Z

*Publisher:*

*Published*

DOI:10.1016/j.measurement.2021.109946

*Terms of use:*

The terms and conditions for the reuse of this version of the manuscript are specified in the publishing policy. The use of copyrighted works requires the consent of the rights' holder (author or publisher). Works made available under a Creative Commons license or a Publisher's custom-made license can be used according to the terms and conditions contained therein. See editor's website for further information and terms and conditions.

This item was downloaded from IRIS Università Politecnica delle Marche (<https://iris.univpm.it>). When citing, please refer to the published version.

(Article begins on next page)

# Development of a measurement setup to detect the level of physical activity and social distancing of ageing people in a social garden during COVID-19 pandemic.

Sara Casaccia<sup>1</sup>, Riccardo Naccarelli<sup>1</sup>, Sara Moccia<sup>2</sup>, Lucia Migliorelli<sup>2</sup>, Emanuele Frontoni<sup>2</sup>, Gian Marco Revel<sup>1</sup>.

<sup>1</sup> Dipartimento di Ingegneria Industriale e Scienze Matematiche, Università Politecnica delle Marche, Ancona.

<sup>2</sup> Dipartimento di Ingegneria dell'Informazione, Università Politecnica delle Marche, Ancona.

E-mail: s.casaccia@univpm.it

Università Politecnica delle Marche, via Brecce Bianche 12, 60131, Ancona.

## Abstract

This study defines a methodology to measure physical activity (PA) in ageing people working in a social garden while maintaining social distancing (SD) during COVID-19 pandemic. A real-time location system (RTLS) with embedded inertial measurement unit (IMU) sensors is used for measuring PA and SD. The position of each person is tracked to assess their SD, finding that the RTLS/IMU can measure the time in which interpersonal distance is not kept with a maximum uncertainty of 1.54 minutes, which compared to the 15-minute limit suggested to reduce risk of transmission at less than 1.5 m, proves the feasibility of the measurement. The data collected by the accelerometers of the IMU sensors are filtered using discrete wavelet transform and used to measure the PA in ageing people with an uncertainty-based thresholding method. PA and SD time measurements were demonstrated exploiting the experimental test in a pilot case with real users.

Keywords: inertial measurement sensors; acceleration signals; discrete wavelet transform; social distancing; physical activity.

## 1. Introduction

Measuring social distancing (SD) during Sars-CoV-2 (COVID-19) pandemic is becoming particularly important especially in contexts where vulnerable individuals could find themselves in contact with potentially infectious people [1]. In these situations, sensors with applied data analytics methods provide measurement systems which can help maintain SD [2]. However, social distancing rules as well as the restrictions imposed by Governments during this pandemic are causing ageing people to become more and more sedentary [3], [4], which has a negative impact on their health and wellbeing [5], [6]. That of encouraging ageing people to maintain SD and still do physical activity (PA) is considered a growing field of research, with many different applications in the area of Ambient Assisted Living (AAL) and wellbeing assessment. In fact, it has been demonstrated that PA affects the ageing process [7] and its monitoring is crucial for the assessment of the quality of life of ageing people [8].

There are several methods for measuring PA [9]. Subjective methods, such as questionnaires and surveys, are inexpensive, but often depend on individual observation and subjective interpretation, making evaluation results inconsistent [10]. Questionnaires are able to capture the PA over a period of time (weeks/months), but have documented limitations including recall bias, especially in older adults [11]. These limitations underscore the importance of objective PA measurement. Various wearable sensors have been developed to objectively measure PA in free-living conditions. Pedometers are the simplest devices for measuring PA. These sensors are able to count the number of steps and to estimate the distance travelled and the expended energy. Furthermore, being inexpensive, portable and lightweight, they are well accepted by users [12]. A strong limitation is due to the inability to record the intensity of the vertical displacement of each step, with the consequence that the estimated energy expended for a run or a walk is the same. Heart rate monitors are an excellent method for measuring the intensity, duration and frequency of PA. They have the benefit of tracking the user's heart rate (HR) during PA [13], with the drawback given by the sensitivity of the HR to emotions and stressful situations, factors that will increase it regardless of PA levels. Heart rate monitoring is used also to estimate the energy expenditure based on the assumption of a linear relationship between HR and oxygen consumption [14]. However, this is only an estimate of calorie expenditure and is prone to error: the person's

age, fitness, gender, and body mass all affect the accuracy of the results. Accelerometers, like pedometers, are small, non-invasive, lightweight, and portable sensors, and they can measure acceleration in gravitational units. The recorded acceleration data are calibrated against measures of known criteria such as energy expenditure, metabolic equivalents (MET) or oxygen consumption [15]. Given the correlation between acceleration data and oxygen consumption, in [16] PA is classified as sedentary, moderate or intense based on published thresholds. Accelerometer data processing algorithms are often proprietary, so users do not have access to the criteria by which PA is classified, although in some cases, sensors allow access to raw data, but these require programming to calculate PA intensity. Recent developments have made it possible to create inertial measurement units (IMUs) consisting of accelerometers, magnetometers, and gyroscope in a single unit. Inertial sensors have therefore become the most used systems to objectively measure PA [17], particularly because they are well accepted both in clinical/laboratory settings and in free living environments [18], [19]. The raw acceleration data measured requires filtering, processing, and computational analysis to provide meaningful measurements. These procedures are applied by the proprietary algorithms of the devices to obtain PA performed and the energy expended. Inertial sensors are used in several research areas of health monitoring, e.g. fall detection [20]–[22], body posture [22] and sport [17]. Moreover, technological advances have led to a decrease in their size and cost while increasing their functionality. These sensors are typically worn on a variety of anatomical positions, but most often on the wrist, being the most accepted place given the most comfortable and least burdensome position [23], [24].

With regards to the monitoring of SD, methods that can be found in literature include the analysis of information acquired from videos of people in urban areas or indoor environments [2] as well as by Bluetooth Low Energy (BLE) [25] or Ultrawide band (UWB) [26] wearables and Global Navigation Satellite System (GNSS) technologies which use smartphones [27].

In this work, ageing people are monitored while attending social garden activities in an outdoor environment to investigate their health and social wellbeing. These activities include all those actions that are usually done inside a garden, such as watering the plants, pruning, digging, raking, harvesting, and sowing. The outdoor environment is a social garden designed and realised for subject over the age of 65 with raised tables to facilitate the gardening activities and avoid pain and overexertion for the seniors. The garden is equipped with non-invasive measurement technologies for the assessment of activity and physiological quantities then stored in a database which was developed in the framework of the SMARTAGE project, as one of the intended measures to support the work of social care cooperatives in the earthquake area of Piceno (Marche Region, Italy). This inner area of central Italy, which was named the “Crater”, was heavily damaged by a series of earthquakes in 2016 as a consequence of which the “Crater” became depopulated. Of its current population 27% is over 65 years old. Therefore, one of the main needs of social care cooperatives working in this area is to create spaces where ageing people can spend time together while attending social activities. For this reason, there is a strong need to support social care cooperatives through the promotion of new business models based on innovative measurement and data analytics technologies. In the social garden here presented ageing people can carry out gardening activities together.

In this context, a user-friendly, non-invasive measurement system able to monitor and analyse PA and SD of ageing people could have a significant impact. There are two different issues that need to be solved at the same time using a low-cost technology: the measurement of PA and the assessment of SD according to COVID-19 prevention rules while users are carrying out activities.

The innovation of this study is the definition and development of a common measurement setup composed of inertial measurement unit (IMU) sensors integrated with a real-time location system (RTLS) network for the acquisition of accelerometer signals and position data of ageing people in the social garden. Once filtered using the discrete wavelet transform (DWT) method to improve accuracy, the accelerometer signals are employed to measure the PA level, for which dedicated metrics are applied. The position data are used to monitor SD according to COVID-19 prevention rules, while assessing the relative uncertainties that are fundamental in the evaluation of a possible risk of infection.

The remaining part of the paper is organised as follow: Section 2 presents the proposed hardware and signal processing for PA and SD monitoring, Section 3 discusses the test results and uncertainty analysis, while Section 4 describes the main conclusions of the paper.

## 2. Materials and methods

### 2.1. Measurement setup

In RTLSs, tags are small electronic devices that are attached to the objects that need to be tracked. In addition to being applied to objects, as in the retail field or in asset tracking, they can also be worn by people who need to be monitored while doing sports [28] or need to receive adequate assistance during daily life [29]. Tags send signals that are received by anchors and then forwarded to a location server that calculates their position. In this study, Tag Leonardo iMU ® by Sewio (dimension: 55x46x17 mm) was used. The technical characteristics of this electronic device are reported in Table 1.

Table 1. Technical characteristics of Tag Leonardo iMU by Sewio.

Components	Usage	Description
Decawave UWB Radio (6500 MHz)	Positioning	Tag emits blinks and RTLS provides precise localization via API. This device has calibration accuracy up to 30 cm in position detection (Tag Leonardo iMU / Personal - Sewio Documentation, <a href="http://www.sewio.net/uwb-tags/">www.sewio.net/uwb-tags/</a> ).
Bluetooth Low Energy	Firmware update	BLE is used for wireless firmware update.
NFC	Configuration	Provides zero-spend energy Tag reconfiguration.
9-axis IMU	Raw data Sensor fusion 3D orientation	Provides raw data (x-y-z axis accelerometer, gyroscope and magnetometer signals) from inertial unit for custom processing like hit/fall detection, jumps etc. or sensor fusion and 3D orientation.
Barometer	z-axis	Provides raw atmospheric pressure data or could be used for direct z-axis estimation.

RTLS use UWB (Ultra-Wide Band) technology to provide precise positioning, in the case presented, of people (Figure 1) through three communication steps:

1. to be tracked, users are equipped with tags that send out a UWB signal to anchors for their localisation,
2. the anchors transmit UWB signals to synchronise with each other,
3. to find users' exact location, a feedback signal from at least 4 anchors must be received. The search for the signal continues until the requirement is satisfied, the data collected by the anchors are then sent to the RTLS server to calculate users' position.

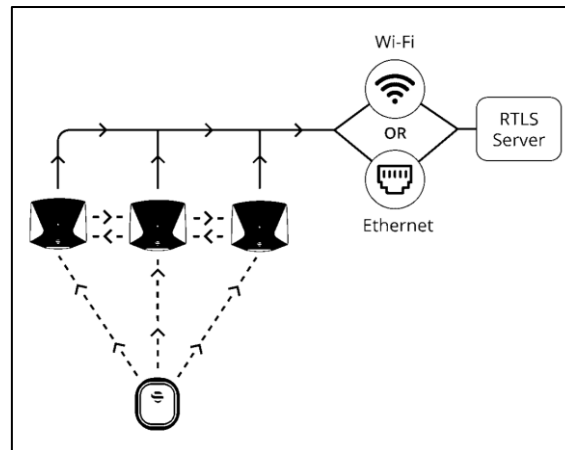


Figure 1. Communication network of the Sewio tracking system.

The experimental setup consisted of six anchor nodes placed around the perimeter of the social garden area, as shown in Figure 2, and the tags worn by the subjects involved in the test, Figure 3. Five ageing people ( $\geq 65$  years old) were involved in the study. The age of the ageing people was chosen based on the SMARTAGE project aim. In fact, the aim of the project is to realise a space where ageing people ( $\geq 65$  years old) could spend time together by doing social activities. The social garden is designed and realised for subject over the age of 65 with raised tables (Figure 4 A) to facilitate the gardening activities and avoid pain and overexertion for the seniors. All the participants involved in the test were volunteer and they gave written informed consent to use their personal data and were duly informed about the goal of the research. Furthermore, a COVID-19 self-declaration form was signed by each subject to prevent the health status of all subjects involved in the test. The conducted study fully respects and promotes the values of freedom, autonomy, integrity and dignity of the person, social solidarity and justice, including fairness of access. The study was carried out in compliance with the principles laid down in the Declaration of Helsinki, in accordance with the Guidelines for Good Clinical Practice. The subjects were asked to carry out activities in the garden while wearing a tag on their dominant wrist for the duration of the test. The wrist was taken as a reference because the activities they were asked to carry out were mainly gardening activities, so they worked mainly with their hands, Figure 4 B, 4 C.

The test consisted in monitoring the subjects while they were at work in the garden. It took place on two different days. Three subjects simultaneously participated in the test on the first day and two on the second.

The data were acquired at 10 Hz. Once sent to the RTLS server, the data were saved in a database to be post-processed to track the positions of the subjects during the test, evaluate their interaction and SD as well as measure the PA performed and the energy expended (EE).



Figure 2. Aerial view of the social garden. The dotted line indicates the perimeter of the garden while the red dots indicate the position of the anchors.

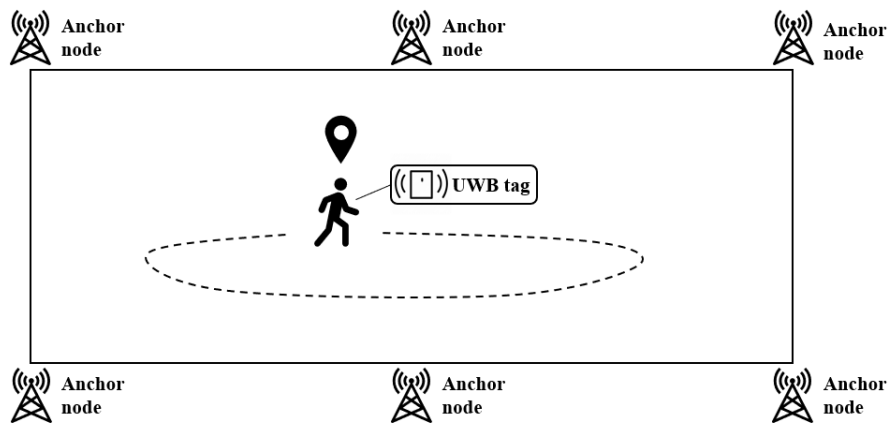


Figure 3. Experimental setup.



Figure 4. A raised table in the social garden (A). Users at work wearing the IMU tag on their dominant wrist (B, C).

## 2.2. Data Processing and Physical activity level assessment

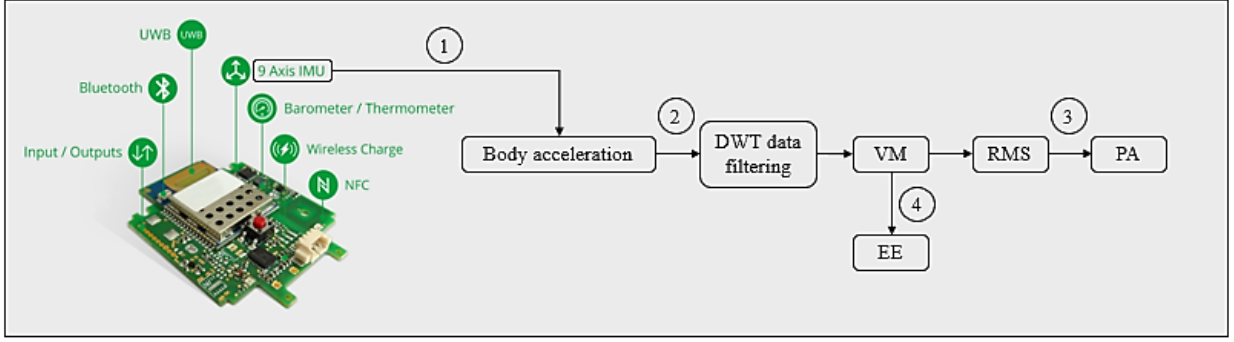


Figure 5. Steps followed to compute the PAL and EE of the subjects from their body acceleration. DWT: discrete wavelet transform; VM: vector magnitude; RMS: root mean square; PA: physical activity; EE: energy expenditure.

To obtain the PA level and EE of the subjects in relation to the activity they carried out during the test, the accelerometric data acquired were processed following four steps (Figure 5):

- Step 1: Accelerations obtained from IMU measurement

The acceleration data recorded by the IMU sensor integrated into the tag placed on the dominant wrist of the subjects, which had a root mean square (RMS) uncertainty of  $1 \text{ m/s}^2$ , were classified along the 3 axes, where the  $x$  and  $y$  axes corresponded to the horizontal plane of the monitoring area and the  $z$  axis to the vertical one. The IMU acceleration data were expressed in the reference frame of the sensor, named  $\overrightarrow{a_{IMU}}$ , at each measure  $i \in [1, n]$  and could be represented as a vector according to the values on the 3 axis of the sensor (Eq. (1)). Thanks to the presence of microelectromechanical components, in addition to the acceleration of the IMU sensor, the measurement of vertical acceleration included gravity ( $g = 9.806 \text{ m/s}^2$ ), so  $g$  was subtracted from the acceleration module along the  $z$  axis (Eq. (2)) as reported in [31]. By doing so, the acceleration that the tag placed on each subject's wrist ( $\overrightarrow{a_{person}}$ ) measured during monitoring was obtained (Eq. (3)).

$$\overrightarrow{a_{IMU}(i)} \left[ \frac{m}{s^2} \right] = [a_{x_{IMU}}(i) \ a_{y_{IMU}}(i) \ a_{z_{IMU}}(i)] \quad (1)$$

$$\overrightarrow{a_{person}(i)} \left[ \frac{m}{s^2} \right] = \overrightarrow{a_{IMU}(i)} - g \vec{z} = [a_{x_{IMU}}(i) \ a_{y_{IMU}}(i) \ a_{z_{IMU}}(i) - g] \quad (2)$$

$$\overrightarrow{a_{person}(i)} \left[ \frac{m}{s^2} \right] = [a_{x_{person}}(i) \ a_{y_{person}}(i) \ a_{z_{person}}(i)] \quad (3)$$

- Step 2: Data filtering using Discrete Wavelet Transform

The accelerometric data were filtered through a denoising procedure using Discrete Wavelet Transform (DWT). The properties of the DWT were employed to recover the original data from the data affected by noise [32], [33], so as not to extract incorrect information. The order 4 Daubechies wavelet was applied to the accelerometric data, obtaining numerically transformed data composed of detailed coefficients and approximate values. To denoise the data, the detailed coefficients were set to zero, and the inverse of the DWT was applied to obtain the original accelerometric noise-free data. An example of a denoised accelerometric signal extract is shown in Figure 6.



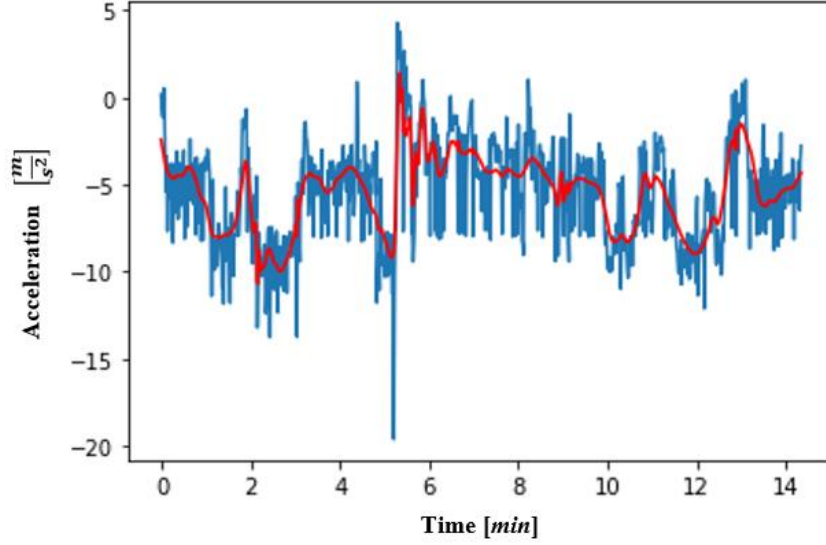


Figure 6. Extract of an accelerometric signal along the x axis (in blue) and its denoised acceleration signal (in red). The denoised signal was obtained by applying the order 4 Daubechies wavelet to the original signal.

- Step 3: Calculation of PA using the uncertainty-based thresholding method

Referring to [34], to compute the PA carried out during the test, the Vector Magnitude (VM) values of each acquired value  $i$  of the accelerations along the 3 axes was calculated [35] through Eq. (4):

$$VM(i) \left[ \frac{m}{s^2} \right] = \sqrt{ax_{person}(i)^2 + ay_{person}(i)^2 + az_{person}(i)^2} \quad (4)$$

Data reduction was applied as reported in [31] by computing the RMS for windows of VM of 30 s (Figure 7).

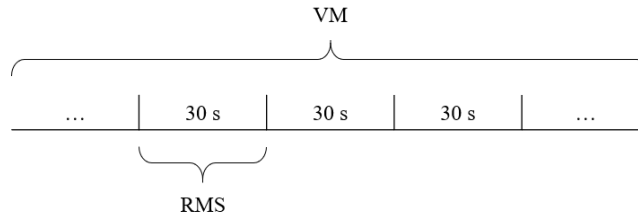


Figure 7. RMS computed for 30 s windows of VM.

According to [36], tasks that involve the use of both the upper and lower body (such as digging, raking) require moderate PA intensity for an old person, while those that involve the use of the upper body while standing or squatting (for example pruning, planting, or harvesting) require low-intensity PA. Considering this, the authors of this study identified PA levels based on the social garden scenario, which was specifically developed to avoid excessive physical strain for its ageing users. Therefore, activities such as standing still were considered as light, activities such as pruning or walking were considered as moderate, while activities such as digging were considered as high. On the basis of the considerations above, to evaluate the PA performed by the subjects, three RMS thresholds that reflect the three PAs identified were set: light, for  $RMS \leq 5 \text{ m/s}^2$ ; medium, for  $5 \text{ m/s}^2 < RMS \leq 11 \text{ m/s}^2$ ; high, for  $RMS > 11 \text{ m/s}^2$ . The RMS threshold values were selected considering as starting point the study of [31], in which the PA performed by young subjects was differentiated into three levels by analysing the accelerometric data acquired through IMUs. Given the RMS threshold values of young subjects in [31] and taking into account a decline in physical strength of approximately 5% per decade [37], the RMS threshold values for ageing subjects were calculated. For the classification of PA, the uncertainty of  $\pm 1 \text{ m/s}^2$  of the IMU sensors was considered. This uncertainty affects the RMS samples that falls between light/medium and medium/high PAs. The authors identified that the PAs could be divided in light, medium and high for the RMS samples that are not affected by the sensor uncertainty and, in addition, light/medium



and medium/high PAs for the RMS samples that would change classification level when the uncertainty interval  $\pm 1 \text{ m/s}^2$  is summed to the measured value. The consequent classification percentage in light, light/medium, medium, medium/high and high PAs was obtained dividing the number of RMS samples falling into each PA level by the total number of samples.

- Step 4: Calculation of total EE

In the last step, the total EE ( $EE_{tot}$ ) value in kcal was computed. The EE at each instant of time (kcal/s) was computed through Eq. (5), as reported in [38], where  $MV$  represents the mean value of the VM assumed during the test. The computed value was then multiplied (Eq. (6)) by the duration of the test in seconds ( $time$ ) to obtain the  $EE_{tot}$ :

$$EE \left[ \frac{kcal}{s} \right] = \left( \frac{4.83 MV + 122.02}{3600} \right) \quad (5)$$

$$EE_{tot} [kcal] = EE \times time \quad (6)$$

### 2.3. Monitoring social distancing

The trajectories performed by each subject during the test were traced based on the acquired data related to their positioning and considering the uncertainty of the system in measuring the coordinates in the test area. The level of interaction between the subjects during the test was then analysed in terms of SD time, which is a particularly critical parameter in this period in which, according to COVID-19 prevention measures, to reduce risk of transmission, people should not stay at a distance of less than 1.5 m for more than 15 minutes. By SD time the authors refer to the time spent by a person at a distance of at least 1.5 m from another person. The Vermont Department of Health considers a close, and therefore dangerous, contact that of people being within 1.5 m of an infectious person for a total of 15 consecutive minutes or more [39]. SD time was calculated for pairs of subjects that simultaneously took part in the test. Even in the case in which more than two subjects are in proximity, the calculation is carried out between each pair of subjects (for example, considering three subjects in proximity, the SD time is evaluated between subjects 1-2, 1-3, 2-3), thus increasing the number of equations. The SD time between each pair was first evaluated by reconstructing the spatial trajectory travelled on the xy plane, taking into account the system's uncertainty ( $\delta$ ) of 30 cm, then by computing the distance between the trajectories and the time of the test in which the trajectories were close ( $< 1.5 \text{ m}$ ) (Eq.(7)). The areas of the social garden where the distancing was not respected were represented by heatmaps, which highlight those areas in which the interaction between users was maximum, therefore highly dangerous.

$$\forall i \quad distance(i) = \sqrt{[(x_1(i) \pm \delta) - (x_2(i) \pm \delta)]^2 + [(y_1(i) \pm \delta) - (y_2(i) \pm \delta)]^2}$$

if  $distance(i) < 1.5 \text{ m}$  then

$$t_{danger}(i) = t_{danger}(i - 1) + 1 \text{ s} \quad (7)$$

where  $x_1(i), y_1(i), x_2(i), y_2(i)$  are the  $i^{th}$  x and y components of the positions recorded by the IMU tag, being the indexes 1 and 2 referred to the two subjects compared, and  $t_{danger}$  is a counter that measures the time in which the two subjects are at a distance of less than 1.5 m from each other. The  $t_{danger}$  counter increments the value obtained in the previous distance comparison ( $t_{danger}(i - 1)$ ) by 1 s each time the proximity condition ( $distance(i) < 1.5 \text{ m}$ ) occurs.

Figure 8 summarises the methodology of tag signal acquisition and processing and shows how it is possible to track trajectories and compute the values of PA and  $EE_{tot}$  from the raw data relating to the subjects' position and acceleration.

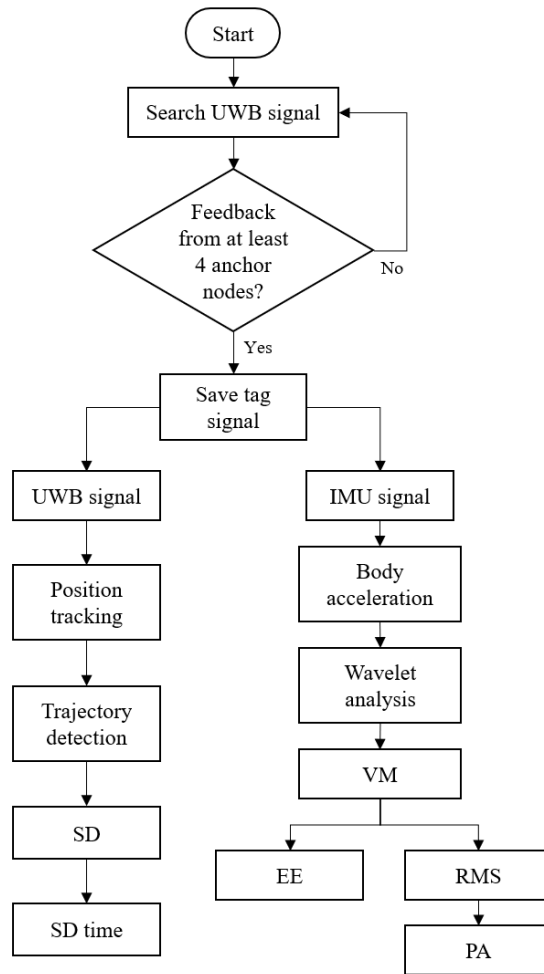
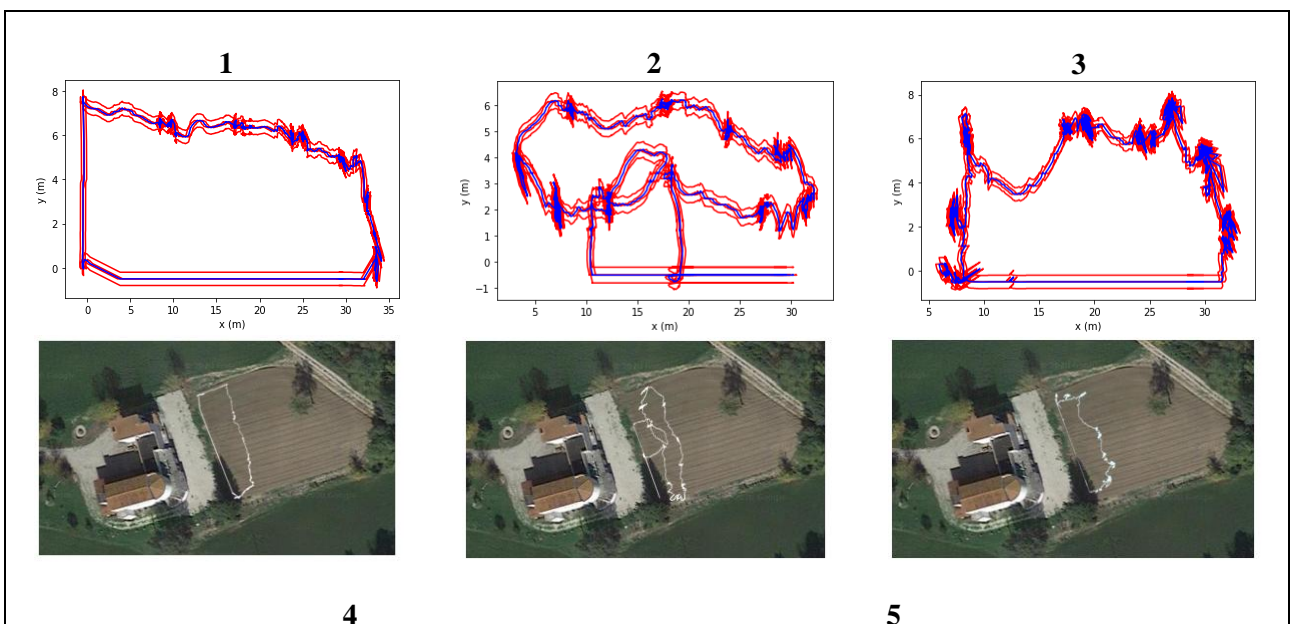


Figure 8. Diagram summarising the steps followed to process the signals acquired by the RTLS/IMU. UWB: ultra-wide band; IMU: inertial measurement unit; VM: vector magnitude; RMS: root mean square; EE: energy expended; PA: physical activity; SD: social distancing.

### 3. Results

Figure 9 shows the trajectories performed by each subject during the test taking into account the uncertainty of the positioning system, which is of 30 cm.



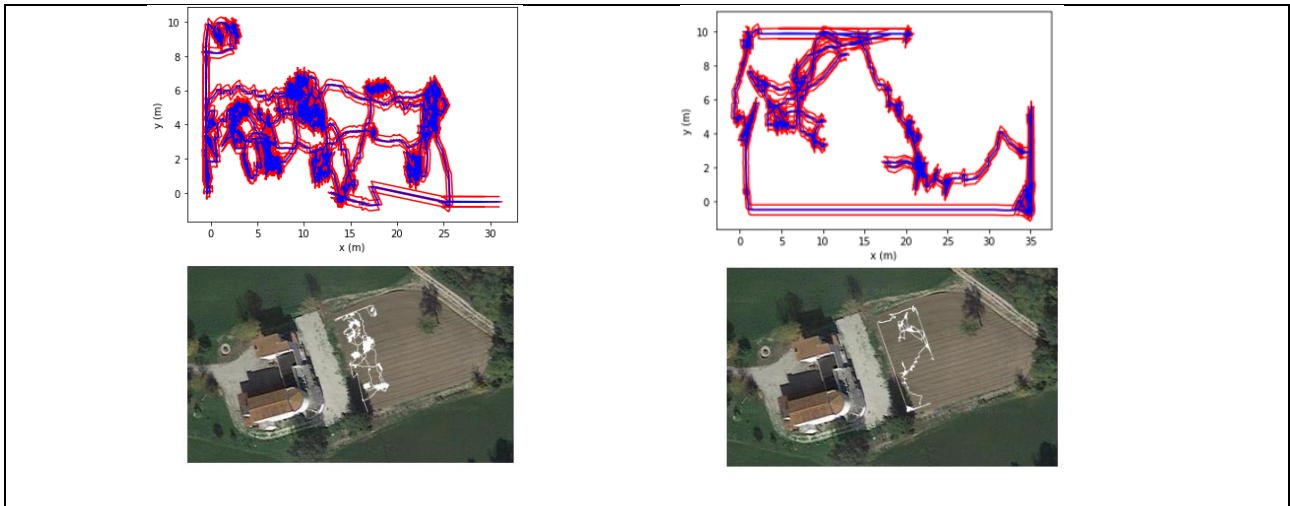


Figure 9. Trajectories performed by each of the subjects during the test (in blue)  $\pm$  uncertainty of the positioning system (in red). For each subject, the map of the social garden on which the subject's trajectory is visible is also reported.

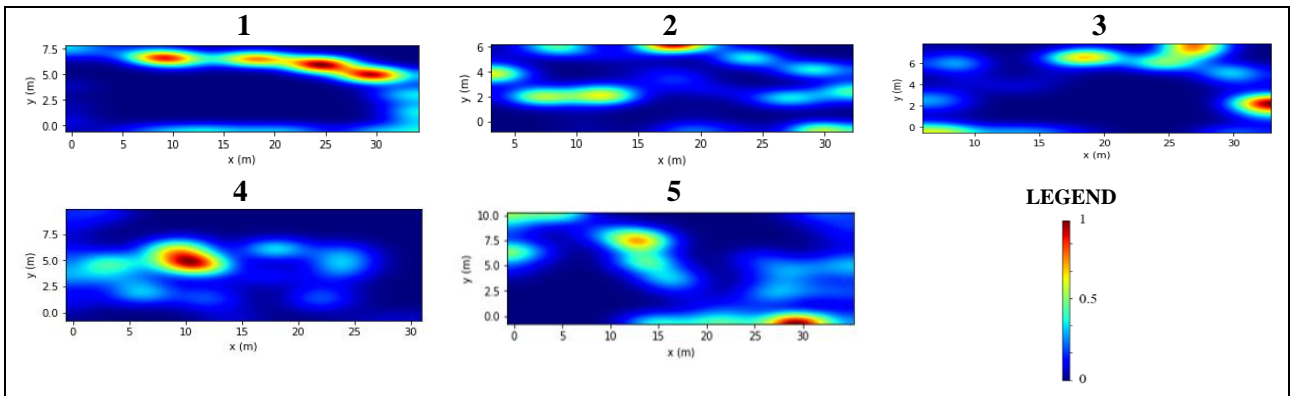


Figure 10. Heatmaps showing the areas of the social garden most frequented by each subject during the test. The legend indicates the colour relating to the state of attendance of a specific area, where 1 is associated with the maximum attendance and 0 with the minimum attendance. The areas shown have different perimeter dimensions due to the different trajectories drawn in the test area.

The heatmaps of Figure 10 are related to the most frequented positions in the test area. They were created knowing the position of each subject. The heatmaps give a two-dimensional representation of the test area as a matrix in which each cell coincides with a portion of the area ( $0.5 \text{ m}^2$ ). Therefore, according to each subjects' attendance of a specific cell, each cell is associated with a value between 0 and 1. The areas most frequented by each subject (values tending to 1) are represented by red cells, while the less frequented ones (values tending to 0) with blue cells.

Table 2 shows the period of time during which the interpersonal distance of 1.5 m between subjects was not respected throughout the test. Considering that the risk of infection is higher when the distance between two subjects is less than 1.5 m for a time of at least 15 minutes, it is important to evaluate how long the subjects found themselves in a similar situation during the test.

Table 2. Time duration of the test in which the distance between the subjects was not respected ( $\pm$  measurement uncertainty).

Compared subjects	Duration of the test in which the interpersonal distance ( $< 1.5 \text{ m}$ ) is not respected [min] $\pm$ uncertainty
1 – 2	$0.76 \pm 0.10$

1 – 3	$3.71 \pm 1.54$
2 – 3	$6.28 \pm 0.57$
4 – 5	$1.62 \pm 0.91$

After assessing how long the subjects were at risk of infection during the test, the areas in which contacts were most relevant were represented, i.e. when users were less than 1.5 m apart. Figure 11, therefore, reports the heatmaps related to the interpersonal distance maintained between each pair of subjects that simultaneously took part in the test. The areas in which the distance between the subjects tended to 0 m (high risk of infection) are shown in red, while the areas in which the distance tended to the limit (1.5 m) suggested according to COVID-19 prevention measures (low risk of infection) are shown in blue.

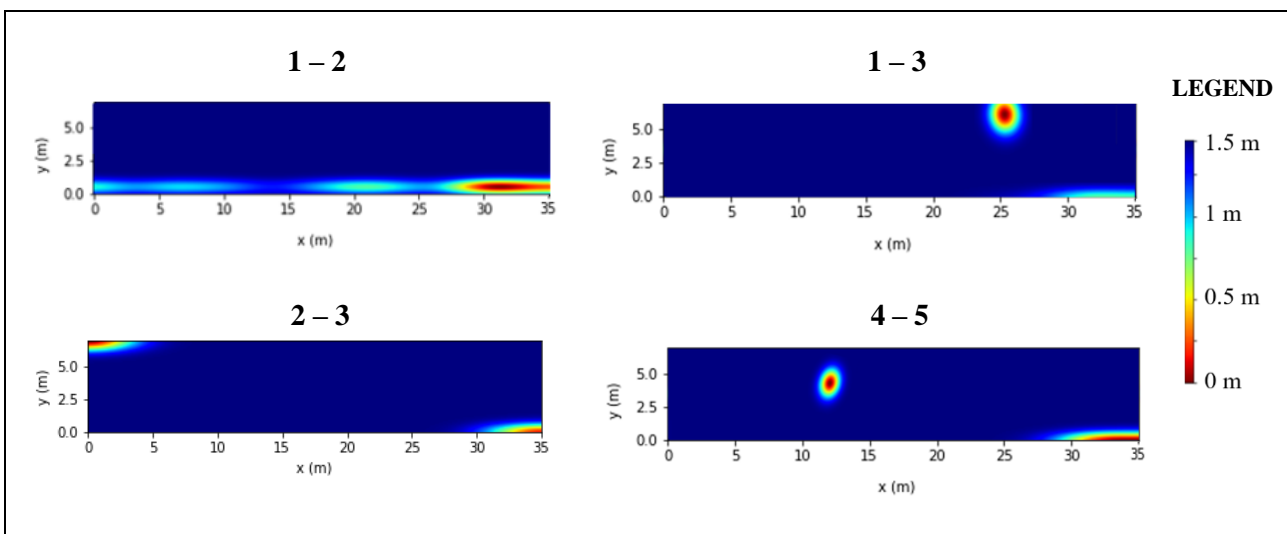
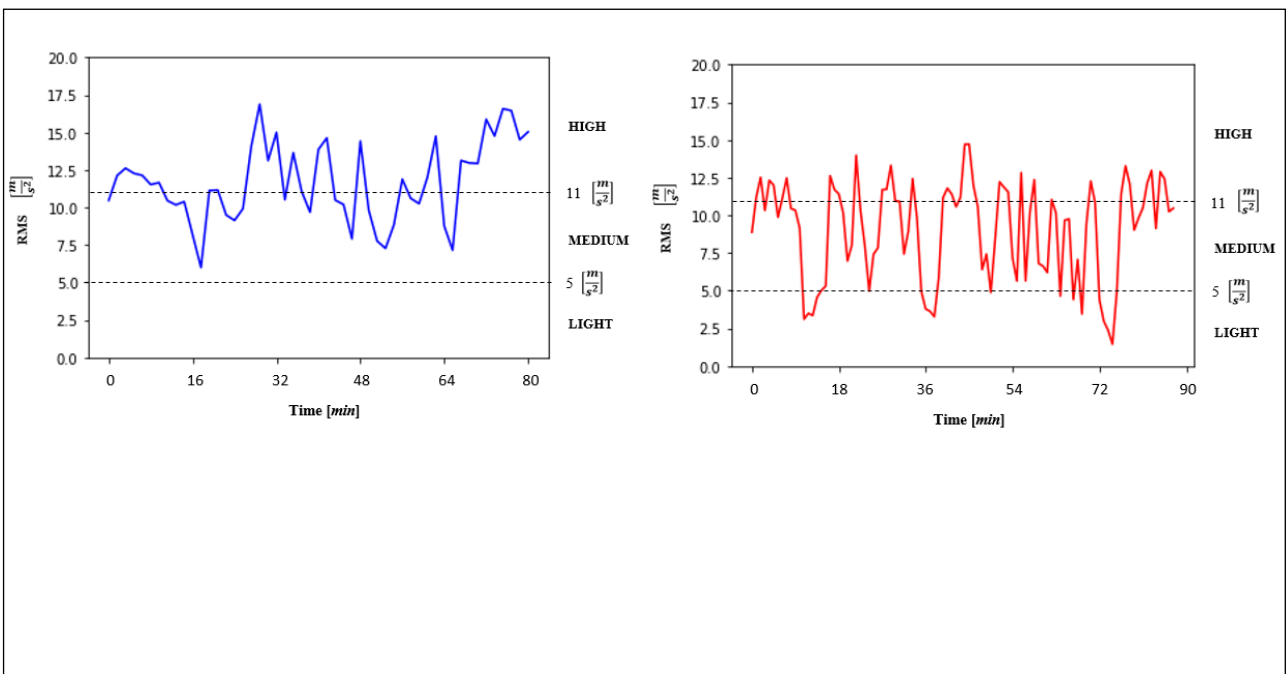


Figure 11. Heatmaps related to the interpersonal distance maintained between the subjects that simultaneously took part the test. The areas in which the distance between the subjects tended to 0 m are shown in red, while the areas in which the distance tended to the limit of 1.5 m suggested according to COVID-19 prevention measures are shown in blue.

Figure 12 reports the PA for each subject evaluated by comparing the RMS values for the duration of the test with the PA thresholds. The black dotted lines represent the thresholds that distinguish light PA from the medium one ( $5 \text{ m/s}^2$ ) and medium PA from the high one ( $11 \text{ m/s}^2$ ).



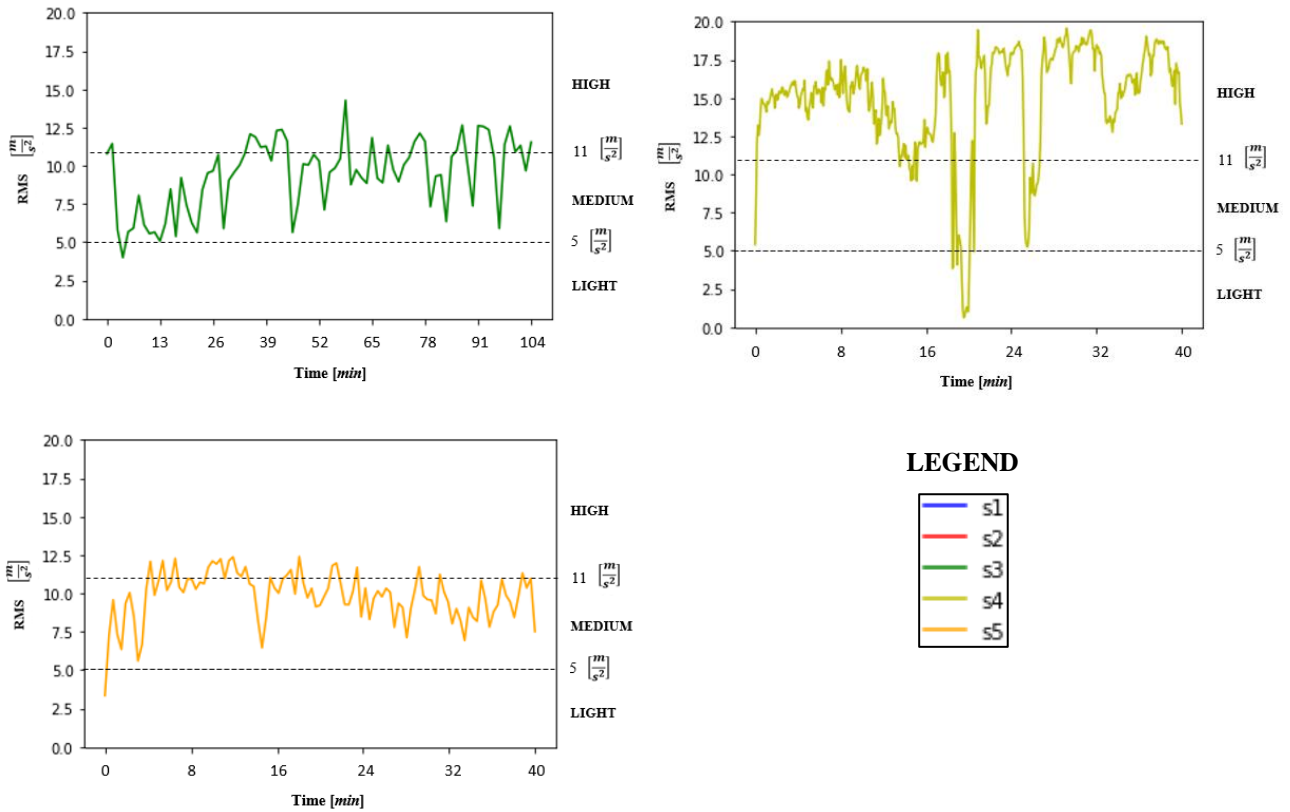


Figure 12. PA for each subject evaluated by comparing the RMS values with the three thresholds set (LIGHT:  $RMS \leq 5 \left[ \frac{m}{s^2} \right]$ ; MEDIUM:  $5 \left[ \frac{m}{s^2} \right] < RMS \leq 11 \left[ \frac{m}{s^2} \right]$ ; HIGH:  $RMS > 11 \left[ \frac{m}{s^2} \right]$ ). The black dotted lines represent the thresholds that distinguish light PA from medium PA ( $5 \left[ \frac{m}{s^2} \right]$ ) and medium PA from high PA ( $11 \left[ \frac{m}{s^2} \right]$ ).

Table 3 shows the day on which the test was carried out, the start and end times, the duration of the test, the percentages of PAs, the mean RMS with the respective associated PA, as well as the  $EE_{tot}$  in kcal related to the duration of the test for each subject. Considering the uncertainty of  $\pm 1 \text{ m/s}^2$  of the IMU sensors, the classification percentage in light, light/medium, medium, medium/high and high PAs are computed dividing the number of RMS samples falling into each PA level by the total number of samples.

Table 3. Day of the test, start and end times, duration of the test, computed percentages of PA related to the duration of the test, uncertainties in PA measurement and  $EE_{tot}$  for each subject.

Subject	Day	Test start - end	Test duration [min]	Percentage of PA	Mean RMS and PA	$EE_{tot}$ [kcal]
1	08-10-2020	-	78	Light: 0%	11.7 m/s <sup>2</sup> - Medium/High	229
				Light/Medium: 2%		
				Medium: 24%		
				Medium/High: 29%		
				High: 45%		

2	08-10-2020	08:16	88	Light: 10%	9.1 m/s <sup>2</sup>	241
		-		Light/Medium: 13%		
		09:44		Medium: 26%		
				Medium/High: 32%		
				High: 19%		
3	08-10-2020	08:16	106	Light:1%	9.4 m/s <sup>2</sup>	295
		-		Light/Medium: 14%		
		10:02		Medium: 37%		
				Medium/High: 36%		
				High:12%		
4	19-10-2020	08:46	40	Light: 2%	14.9 m/s <sup>2</sup>	127
		-		Light/Medium: 3%		
		09:26		Medium: 4%		
				Medium/High: 5%		
				High: 86%		
5	19-10-2020	08:46	40	Light: 1%	9.8 m/s <sup>2</sup>	111
		-		Light/Medium: 1%		
		09:26		Medium: 46%		
				Medium/High: 44%		
				High: 8%		

#### 4. Discussion and conclusions

The goal of this work is based on the need of monitoring physical activity in ageing people since it is one of the most important things to do for health. Performing PA during this time when the COVID-19 pandemic requires maintaining interpersonal distancing is a problem [40] that can be solved by monitoring SD while performing PA. In this context, the aim of this study is to present an innovative data measurement and analysis method for assessing the PA level of ageing people while maintaining social distancing during the COVID-19 pandemic. This study is conducted as part of the SMARTAGE project, which aims to create a space where ageing people can spend time together carrying out social activities. The hypothesis of the study is the definition of a non-invasive measurement methodology for the assessment of the PA and SD based on remote user monitoring, which ensures data anonymization and privacy.

Using a commercially available tracking system composed of a RTLS with an embedded IMU sensor, five ageing people were monitored in an innovative scenario: the social garden. The position of each subject measured from the tracking system was used to know their movements to assess whether each subject

maintained the social distancing suggested by COVID-19 prevention rules. The time intervals during the test in which the interpersonal distance of 1.5 m between each pair of subjects that simultaneously took part in the test was not respected was measured.

Considering the RTLS uncertainty of 30 cm in the position measurement, the maximum uncertainty of the system in the measurement of the time in which SD was not respected is 1.54 min. As it can be seen from the results, the temporal values of interaction between the users during the test were limited and in any case below 15 minutes, which is the period of exposure considered at risk. This demonstrates that social distancing was respected throughout the test. Although some of the uncertainties in percentage have a considerable weight in determining the time intervals during the test in which the safety distance was not respected, if compared to the 15 minute-limit they are still not relevant quantities.

Besides location detection, the tracking system, which is provided with an embedded IMU sensor, was used for measuring the acceleration signals from the subjects' wrists, which were then processed to measure the PA of the subjects in the garden. Currently there are no studies that compare the effects of different window lengths for ageing people. In the study here presented the authors chose to calculate the RMS values for windows of VM of 30 s, considering this interval a suitable time window for evaluating changes in physical activity. To assess the PA, it was then necessary to define an uncertainty-based thresholding method setting RMS thresholds that reflected in the classification of PAs. RMS values  $\leq 5 \text{ m/s}^2$  were assigned to light PA, RMS values between  $5 \text{ m/s}^2$  and  $11 \text{ m/s}^2$  to medium PA, while RMS values  $> 11 \text{ m/s}^2$  to high PA. The uncertainty of  $\pm 1 \text{ m/s}^2$  of the IMU sensors was then considered for the classification of PAs and the consequent classification percentage in light, light/medium, medium, medium/high and high PAs was computed.

The uncertainty-based thresholding method was defined in order to establish PAs that reflected the intensity of the work done by the subjects in the garden also considering the uncertainty of the IMU sensors. For this reason, in setting these values, the authors took into account the age of the subjects as well as the fact that the fatigue threshold is lower in an ageing person than in a young/adult subject. According to the results obtained, the subjects carried out mostly medium and high gardening activities, since they mostly walked or did gardening work such as pruning and digging.

The last phase of the analysis consisted in the calculation of the total energy spent during the monitoring. Table 3 shows the percentage of PA related to the duration of the test for each subject together with the associated total energy spent.

In conclusion, this work demonstrated the possibility of measuring the PA of ageing people and their SD time within the social garden scenario by using a sensor network consisting of a RTLS with embedded IMU sensors. The uncertainty seems to be compatible with the requirements for the application. The proposed methodology is suitable to be applied in many different contexts, ranging from working/construction sites to sport facilities.

#### 4.1. Limitations and strengths

Since this work deals with the development of a measurement system to non-invasively and remotely measure the PA and SD of ageing people in a social garden scenario, limitations and strength are presented in this section. Technological limits have been introduced by the measurement system concerning the uncertainty of the positioning system of 30 cm and the uncertainty of  $1 \text{ m/s}^2$  of the IMU sensor. The uncertainty of the positioning system was demonstrated to be acceptable considering the maximum uncertainty of 1.54 minutes found in this work in measuring interpersonal distance time, while the uncertainty of  $1 \text{ m/s}^2$  of the IMU sensor resulted in the identification of five PA levels instead of three. Furthermore, limitations are also focused on the cost of the measurement system composed by anchors and tags instrumentation. In the specific scenario of the social garden, the cost is well covered by the social care organization, but this measurement system could become expensive if the scenario includes more than one perimeter of investigation. In fact, this measurement system is already used in malls to monitor the shopping trolley routes [41] or in sport facilities where the outputs can be used to increase the business model of the facility [42]. The same measurement system is not



suggested to be installed in private environments where more than one room needs to be monitored to extract information regarding the behaviour of the residents. Moreover, a limitation on the use of wearables, i.e. tags worn by the ageing people on the wrist, could be identified due to user acceptance [43]. Since the wearable tag is worn for a short time in this scenario, the wearable is well accepted by the involved subjects. On the other hand, this work presents some strengths. In particular, the privacy of the user is respected by using this measurement system guarantying the data anonymization. A context that can certainly benefit from the use of this type of system is long-term care setting. The application of RTLS technology can in fact be used in the patient/resident assistance process for the measurement of their physical activity and social interaction. In this scenario, the monitoring system can be installed within the common environment in the long-term care setting, which represents the fulcrum of social life where residents gather to carry out most of the activities. The caregivers are thus able to monitor each resident via the RTLS platform, which reports their state of physical activity and level of social interaction, so that they can check if there is a significant change in seniors' routines.

## Acknowledgements

The authors wish to thank the partners of the SMARTAGE project and gratefully acknowledge the support of the Marche Region in funding the project in the framework of the POR MARCHE FESR 2014-2020 Programme. The authors also thank the coordinator of the project, the social cooperative "Lella 2001 Onlus".

## References

- [1] Z. Vokó and J. G. Pitter, 'The effect of social distance measures on COVID-19 epidemics in Europe: an interrupted time series analysis', *GeroScience*, vol. 42, no. 4, pp. 1075–1082, Aug. 2020, doi: 10.1007/s11357-020-00205-0.
- [2] C. V. Niño Rondón *et al.*, 'Video image processing to verify social distancing during the COVID-19 pandemic', *Rev. Logos Cienc. Amp Tecnol.*, vol. 13, no. 1, pp. 116–127, Apr. 2021, doi: 10.22335/rlct.v13i1.1305.
- [3] A. Rutkowska, K. Kacperak, S. Rutkowski, L. Cacciante, P. Kiper, and J. Szczegielniak, 'The Impact of Isolation Due to COVID-19 on Physical Activity Levels in Adult Students', *Sustainability*, vol. 13, no. 2, Art. no. 2, Jan. 2021, doi: 10.3390/su13020446.
- [4] K. Yamada, S. Yamaguchi, K. Sato, T. Fuji, and T. Ohe, 'The COVID-19 outbreak limits physical activities and increases sedentary behavior: A possible secondary public health crisis for the elderly', *J. Orthop. Sci.*, vol. 25, no. 6, pp. 1093–1094, Nov. 2020, doi: 10.1016/j.jos.2020.08.004.
- [5] F. B. Schuch *et al.*, 'Moderate to vigorous physical activity and sedentary behavior changes in self-isolating adults during the COVID-19 pandemic in Brazil: a cross-sectional survey exploring correlates', *Sport Sci. Health*, Jun. 2021, doi: 10.1007/s11332-021-00788-x.
- [6] M. Kimura, T. Ojima, K. Ide, and K. Kondo, 'Allaying Post-COVID 19 Negative Health Impacts Among Older People: The "Need To Do Something With Others"—Lessons From the Japan Gerontological Evaluation Study', *Asia Pac. J. Public Health*, vol. 32, no. 8, pp. 479–484, Nov. 2020, doi: 10.1177/1010539520951396.
- [7] B. Langhammer, A. Bergland, and E. Rydwick, 'The Importance of Physical Activity Exercise among Older People', *BioMed Res. Int.*, vol. 2018, p. 7856823, 2018, doi: 10.1155/2018/7856823.
- [8] R. Sawatzky, T. Liu-Ambrose, W. C. Miller, and C. A. Marra, 'Physical activity as a mediator of the impact of chronic conditions on quality of life in older adults', *Health Qual. Life Outcomes*, vol. 5, p. 68, Dec. 2007, doi: 10.1186/1477-7525-5-68.
- [9] R. J. Shephard and Y. Aoyagi, 'Measurement of human energy expenditure, with particular reference to field studies: an historical perspective', *Eur. J. Appl. Physiol.*, vol. 112, no. 8, pp. 2785–2815, Aug. 2012, doi: 10.1007/s00421-011-2268-6.
- [10] G. A. Meijer, K. R. Westerterp, F. M. Verhoeven, H. B. Koper, and F. ten Hoor, 'Methods to assess physical activity with special reference to motion sensors and accelerometers', *IEEE Trans. Biomed. Eng.*, vol. 38, no. 3, pp. 221–229, Mar. 1991, doi: 10.1109/10.133202.
- [11] A. K. Rao, 'Wearable Sensor Technology to Measure Physical Activity (PA) in the Elderly', *Curr. Geriatr. Rep.*, vol. 8, no. 1, pp. 55–66, Mar. 2019, doi: 10.1007/s13670-019-0275-3.

- [12] N. F. Butte, U. Ekelund, and K. R. Westerterp, 'Assessing Physical Activity Using Wearable Monitors: Measures of Physical Activity', *Med. Sci. Sports Exerc.*, vol. 44, no. 1S, pp. S5–S12, Jan. 2012, doi: 10.1249/MSS.0b013e3182399c0e.
- [13] S. J. Hensen, 'Measuring Physical Activity With Heart Rate Monitors', *Am. J. Public Health*, vol. 107, no. 12, p. e24, Dec. 2017, doi: 10.2105/AJPH.2017.304121.
- [14] A. P. Hills, N. Mokhtar, and N. M. Byrne, 'Assessment of Physical Activity and Energy Expenditure: An Overview of Objective Measures', *Front. Nutr.*, vol. 1, Jun. 2014, doi: 10.3389/fnut.2014.00005.
- [15] B. Ainsworth, L. Cahalin, M. Buman, and R. Ross, 'The Current State of Physical Activity Assessment Tools', *Prog. Cardiovasc. Dis.*, vol. 57, no. 4, pp. 387–395, Jan. 2015, doi: 10.1016/j.pcad.2014.10.005.
- [16] P. Freedson, H. R. Bowles, R. Troiano, and W. Haskell, 'Assessment of Physical Activity Using Wearable Monitors: Recommendations for Monitor Calibration and Use in the Field', *Med. Sci. Sports Exerc.*, vol. 44, no. 1S, p. S1, Jan. 2012, doi: 10.1249/MSS.0b013e3182399b7e.
- [17] C. Crema, A. Depari, A. Flammini, E. Sisinni, T. Haslwanter, and S. Salzmänn, 'Characterization of a wearable system for automatic supervision of fitness exercises', *Measurement*, vol. 147, p. 106810, Dec. 2019, doi: 10.1016/j.measurement.2019.07.038.
- [18] A. Doherty *et al.*, 'Large Scale Population Assessment of Physical Activity Using Wrist Worn Accelerometers: The UK Biobank Study', *PLOS ONE*, vol. 12, no. 2, p. e0169649, Feb. 2017, doi: 10.1371/journal.pone.0169649.
- [19] M. J. Mathie, A. C. F. Coster, N. H. Lovell, and B. G. Celler, 'Accelerometry: providing an integrated, practical method for long-term, ambulatory monitoring of human movement', *Physiol. Meas.*, vol. 25, no. 2, pp. R1–20, Apr. 2004, doi: 10.1088/0967-3334/25/2/r01.
- [20] L. Chen, R. Li, H. Zhang, L. Tian, and N. Chen, 'Intelligent fall detection method based on accelerometer data from a wrist-worn smart watch', *Measurement*, vol. 140, pp. 215–226, Jul. 2019, doi: 10.1016/j.measurement.2019.03.079.
- [21] P. V. Er and K. K. Tan, 'Non-intrusive fall detection monitoring for the elderly based on fuzzy logic', *Measurement*, vol. 124, pp. 91–102, Aug. 2018, doi: 10.1016/j.measurement.2018.04.009.
- [22] F. Lamonaca, G. Polimeni, K. Barbé, and D. Grimaldi, 'Health parameters monitoring by smartphone for quality of life improvement', *Measurement*, vol. 73, pp. 82–94, Sep. 2015, doi: 10.1016/j.measurement.2015.04.017.
- [23] D. Arvidsson, J. Fridolfsson, and M. Börjesson, 'Measurement of physical activity in clinical practice using accelerometers', *J. Intern. Med.*, vol. 286, no. 2, pp. 137–153, 2019, doi: <https://doi.org/10.1111/joim.12908>.
- [24] J. J. Scott, A. V. Rowlands, D. P. Cliff, P. J. Morgan, R. C. Plotnikoff, and D. R. Lubans, 'Comparability and feasibility of wrist- and hip-worn accelerometers in free-living adolescents', *J. Sci. Med. Sport*, vol. 20, no. 12, pp. 1101–1106, Dec. 2017, doi: 10.1016/j.jsams.2017.04.017.
- [25] M. Fazio, A. Buzachis, A. Galletta, A. Celesti, and M. Villari, 'A proximity-based indoor navigation system tackling the COVID-19 social distancing measures', in *2020 IEEE Symposium on Computers and Communications (ISCC)*, Jul. 2020, pp. 1–6. doi: 10.1109/ISCC50000.2020.9219634.
- [26] Y. Cao, A. Dhekne, and M. Ammar, '6Fit-A-Part: A Protocol for Physical Distancing on a Custom Wearable Device', in *2020 IEEE 28th International Conference on Network Protocols (ICNP)*, Oct. 2020, pp. 1–12. doi: 10.1109/ICNP49622.2020.9259374.
- [27] A. Ksentini and B. Brik, 'An Edge-Based Social Distancing Detection Service to Mitigate COVID-19 Propagation', *IEEE Internet Things Mag.*, vol. 3, no. 3, pp. 35–39, Sep. 2020, doi: 10.1109/IOTM.0001.2000138.
- [28] R. Leser, A. Baca, and G. Ogris, 'Local Positioning Systems in (Game) Sports', *Sensors*, vol. 11, no. 10, Art. no. 10, Oct. 2011, doi: 10.3390/s111009778.
- [29] J. (Joost) van Hoof *et al.*, 'Real-time Location Systems for Asset Management in Nursing Homes', De Haagse Hogeschool, 2018.
- [30] 'Tag Leonardo iMU / Personal - Sewio Documentation'. <https://docs.sewio.net/docs/tag-leonardo-imu-personal-3244761.html> (accessed Jan. 18, 2021).
- [31] F. Marin, K. Lepetit, L. Fradet, C. Hansen, and K. Ben Mansour, 'Using accelerations of single inertial measurement units to determine the intensity level of light-moderate-vigorous physical activities: Technical and mathematical considerations', *J. Biomech.*, vol. 107, p. 109834, May 2020, doi: 10.1016/j.jbiomech.2020.109834.
- [32] T. S. Edwards, 'An improved wavelet correction for zero shifted accelerometer data', *Shock Vib.*, vol. 10, no. 3, pp. 159–167, Jan. 2003.

- [33] R. Madan and S. Kr, 'Signal Filtering Using Discrete Wavelet Transform', *Int J Recent Trends Eng*, vol. 2, Jan. 2009.
- [34] V. T. van Hees *et al.*, 'Estimation of daily energy expenditure in pregnant and non-pregnant women using a wrist-worn tri-axial accelerometer', *PloS One*, vol. 6, no. 7, p. e22922, 2011, doi: 10.1371/journal.pone.0022922.
- [35] F. Pietroni, S. Casaccia, G. M. Revel, and L. Scalise, 'Methodologies for continuous activity classification of user through wearable devices: Feasibility and preliminary investigation', in *2016 IEEE Sensors Applications Symposium (SAS)*, Apr. 2016, pp. 1–6. doi: 10.1109/SAS.2016.7479867.
- [36] S.-A. Park, K.-S. Lee, and K.-C. Son, 'Determining Exercise Intensities of Gardening Tasks as a Physical Activity Using Metabolic Equivalents in Older Adults', *HortScience*, vol. 46, no. 12, pp. 1706–1710, Dec. 2011, doi: 10.21273/HORTSCI.46.12.1706.
- [37] Z. Milanović, S. Pantelić, N. Trajković, G. Sporiš, R. Kostić, and N. James, 'Age-related decrease in physical activity and functional fitness among elderly men and women', *Clin. Interv. Aging*, vol. 8, pp. 549–556, 2013, doi: 10.2147/CIA.S44112.
- [38] I. M. Pires, V. Felizardo, N. Pombo, M. Drobnics, N. M. Garcia, and F. Flórez-Revuelta, 'Validation of a method for the estimation of energy expenditure during physical activity using a mobile device accelerometer', *J. Ambient Intell. Smart Environ.*, vol. 10, no. 4, pp. 315–326, Jan. 2018, doi: 10.3233/AIS-180494.
- [39] J. C. Pringle, 'COVID-19 in a Correctional Facility Employee Following Multiple Brief Exposures to Persons with COVID-19 — Vermont, July–August 2020', *MMWR Morb. Mortal. Wkly. Rep.*, vol. 69, 2020, doi: 10.15585/mmwr.mm6943e1.
- [40] T. S. Matias and F. H. Dominski, 'The COVID-19 pandemic challenges physical activity with two emerging paradigms', *Rev. Bras. Atividade Física Saúde*, vol. 25, pp. 1–6, Sep. 2020, doi: 10.12820/rbafs.25e0113.
- [41] N. Ferracuti, C. Norscini, E. Frontoni, P. Gabellini, M. Paolanti, and V. Placidi, 'A business application of RTLS technology in Intelligent Retail Environment: Defining the shopper's preferred path and its segmentation', *J. Retail. Consum. Serv.*, vol. 47, pp. 184–194, Mar. 2019, doi: 10.1016/j.jretconser.2018.11.005.
- [42] G. Ferrer, N. Dew, and U. Apte, 'When is RFID right for your service?', *Int. J. Prod. Econ.*, vol. 124, no. 2, pp. 414–425, Apr. 2010, doi: 10.1016/j.ijpe.2009.12.004.
- [43] S. Farivar, M. Abouzahra, and M. Ghasemaghaei, 'Wearable device adoption among older adults: A mixed-methods study', *Int. J. Inf. Manag.*, vol. 55, p. 102209, Dec. 2020, doi: 10.1016/j.ijinfomgt.2020.102209.